IAI Journals.ASM.org

Role of CD11b/CD18 in the Process of Intoxication by the Adenylate Cyclase Toxin of *Bordetella pertussis*

Joshua C. Eby, Mary C. Gray, Annabelle R. Mangan,* Gina M. Donato, and Erik L. Hewlett

Division of Infectious Diseases and International Health, Department of Medicine, University of Virginia School of Medicine, Charlottesville, Virginia, USA

The adenylate cyclase toxin (ACT) of *Bordetella pertussis* does not require a receptor to generate intracellular cyclic AMP (cAMP) in a broad range of cell types. To intoxicate cells, ACT binds to the cell surface, translocates its catalytic domain across the cell membrane, and converts intracellular ATP to cAMP. In cells that express the integrin CD11b/CD18 (CR3), ACT is more potent than in CR3-negative cells. We find, however, that the maximum levels of cAMP accumulation inside CR3-positive and -negative cells are comparable. To better understand how CR3 affects the generation of cAMP, we used Chinese hamster ovary and K562 cells transfected to express CR3 and examined the steps in intoxication in the presence and absence of the integrin. The binding of ACT to cells is greater in CR3-expressing cells at all concentrations of ACT, and translocation of the catalytic domain is enhanced by CR3 expression, with ~80% of ACT molecules translocating their catalytic domain in CR3-positive cells but only 25% in CR3-negative cells. Once in the cytosol, the unregulated catalytic domain converts ATP to cAMP, and at ACT concentrations >1,000 ng/ml, the intracellular ATP concentration is <5% of that in untreated cells, regardless of CR3 expression. This depletion of ATP prevents further production of cAMP, despite the CR3-mediated enhancement of binding and translocation. In addition to characterizing the effects of CR3 on the actions of ACT, these data show that ATP consumption is yet another concentration-dependent activity of ACT that must be considered when studying how ACT affects target cells.

The adenylate cyclase toxin (ACT) of *Bordetella pertussis*, the causative agent of whooping cough, is a single polypeptide composed of an N-terminal, 400-amino-acid adenylate cyclase (AC) enzymatic domain and a 1,306-amino-acid cell-binding domain homologous to the repeats-in-toxin (RTX) family of calcium-binding, pore-forming bacterial protein toxins (2, 16, 17, 26, 32). The AC domain converts ATP to cAMP in a high-turnover reaction that is stimulated by eukaryotic calmodulin (18). The RTX component forms oligomeric pores in cell membranes and serves as the cell binding domain (55, 58). To generate cyclic AMP (cAMP), ACT binds to cells, translocates the catalytic domain across the cytoplasmic membrane without endocytosis or macropinocytosis (11, 19, 25), and catalyzes the conversion of intracellular ATP to cAMP.

Several cytotoxic effects for ACT have been identified, starting with the discovery that toxin-generated cAMP inhibits core functions of neutrophils and macrophages, such as the generation of an oxidative burst and killing of phagocytized bacteria (8, 49). ACT elicits additional cAMP-mediated effects in a variety of eukaryotic cells; these include apoptotic cell death, dysfunction of the cell cytoskeleton, cell cycle arrest, chloride secretion from polarized epithelial cells, and dysregulation of the adaptive immune system (8, 11, 22, 30, 34, 47, 49, 50, 54). To generate cAMP, the AC enzyme reaction consumes cellular ATP, further contributing to toxin-mediated cytotoxicity (4, 28). The pore-forming, RTX component of the toxin molecule synergizes with the ACT-generated, supraphysiologic levels of cAMP and concomitant ATP depletion to promote nonapoptotic death of macrophages (1, 4, 28).

During the 35 years since its discovery, ACT has been observed to affect multiple cell types over a broad range of concentrations *in vitro* (8, 27, 34, 49). ACT also produces ion-conducting channels across artificial lipid bilayers and elicits marker release from multilamellar liposomes containing no protein (5, 20, 38, 40, 55). Collectively, these data suggested that there is not a specific receptor required for ACT to affect target cells. In 2001, however, Guermonprez et al. discovered that the expression of the β_2 integrin CD11b/CD18 (CR3) enhances the sensitivity of cells to intoxication (24). Subsequently, El-Azami-El-Idrissi et al. demonstrated that the posttranslational acylation of the toxin is required for tight, efficient binding of ACT to CR3 and that a segment of the RTX repeats (amino acids 1166 to 1281) is involved in that interaction (13).

That ACT affects cells with and without CR3 raises the question, "What is the contribution of CR3 to intoxication of eukaryotic cells by ACT?" To address this question, we have characterized the effects of CR3 on the steps leading to intoxication: binding of ACT to the target cell, translocation of the catalytic domain directly across the cytoplasmic membrane, and production of cAMP by the internalized AC enzymatic component. We have found that CR3 enhances the binding and translocation of the toxin but that the effect of CR3 on intracellular cAMP generation is limited by the depletion of ATP that occurs during the AC enzymatic reaction. Because the ATP concentration limits the amount of cAMP that can be made, there is excess toxin bound to CR3-positive ($CR3^+$) cells that does not produce cAMP. ACT-induced ATP consumption, which is concentration dependent and which occurs in cells with and without CR3, should therefore

Received 28 September 2011 **Returned for modification** 24 October 2011
Accepted 18 November 2011

Published ahead of print 5 December 2011

Editor: S. R. Blanke

Address correspondence to Erik L. Hewlett, eh2v@virginia.edu.

* Present address: Virginia Tech Carilion School of Medicine and Research Institute, Roanoke, Virginia, USA.

doi:10.1128/IAI.05979-11

be considered when interpreting studies regarding the mechanism and effects of ACT.

MATERIALS AND METHODS

Materials. All reagents, unless otherwise stated, were purchased from Sigma Chemical Co. (St. Louis, MO). Rabbit polyclonal immunoglobulin to ACT was produced by Covance laboratories and purified by Gamma-Bind Plus Sepharose (GE Healthcare Life Sciences). Monoclonal antibody (MAb) to CD11b (M1/70), isotype control, and fluorescein isothiocyanate (FITC)-conjugated MAb to CD18 (clone 6.7) were purchased from BD Pharmingen. Phycoerythrin (PE)-conjugated monoclonal antibody to CD11b, clone ICRF44, and streptavidin-conjugated allophycocyanin (APC) were purchased from BioLegend. The biotin conjugation kit was purchased from Invitrogen. Cell dissociation buffer was purchased from Gibco.

Production and purification of AC toxin. *Escherichia coli* XL-1 Blue cells (Stratagene, La Jolla, CA) containing the appropriate plasmid construct (wild-type [WT] ACT or inactive ACT) were used for toxin production as previously described (23, 29). Cultured bacteria were centrifuged, and the resulting pellet was resuspended in 50 mM Tris (pH 7.5), sonicated, and extracted with 8 M urea. Urea-extracted ACT was purified on a DEAE ion-exchange column and a calmodulin affinity column as described previously (35). ACT was stored at −80°C in 8 M urea, 10 mM tricine, 0.5 mM EDTA, 0.5 mM EGTA, pH 8.0.

Cell culture. CHO-K1 cells stably transfected to express CD11b and CD18 (CHO $CR3^+$) or stably mock transfected with a neomycin resistance vector as control (CHO) were obtained as a kind gift from Douglas Golenbock and grown as described previously (31). K562 cells stably transfected to express CD11b and CD18 (K562 $CR3^+$) or K562 control cells (K562) were kind gifts of Li Zhang and were established and maintained as described previously (59). Surface expression of CD11b and CD18 was monitored by flow cytometry intermittently during the experiments to ensure stable coexpression using PE-conjugated MAb ICRF44 to CD11b and FITC-conjugated MAb 6.7 to CD18. The expression of CD11b in CHO and K562 cells is shown in Fig. 3D and E. J774 cells, a murine macrophage cell line, were cultured in Dulbecco's modified Eagle medium (DMEM) with high glucose (Gibco) and 10% heat-inactivated fetal bovine serum (FBS-HI). BEAS-2B cells, a normal human bronchial epithelial cell line, immortalized by adenovirus 12 and simian virus 40 (Ad12-SV40) transformation, were purchased from ATCC and cultured according to the manufacturer's instructions in complete BEGM (Lonza) containing all the supplied supplements except GA-1000 (gentamicin-amphotericin B). Cells were grown in tissue culture flasks precoated with 0.01 mg/ml bovine fibronectin (Calbiochem), 0.03 mg/ml bovine collagen type I (BD Biosciences), and 0.01 mg/ml bovine serum albumin prepared in basal BEBM (Lonza). All cells were grown at 37°C in 5% CO_2.

Measurement of intracellular cAMP. Approximately 24 h before the start of experiments, CHO and J774 cells were plated at 30,000 to 40,000 per well in 96-well tissue culture plates. BEAS-2B cells were seeded at 60,000/well in precoated wells and grown overnight in complete BEGM. Immediately before experiments using CHO or J774 cells, the growth medium was removed and replaced with Hank's balanced salt solution (Gibco) with 0.1% human albumin (HBSS-HA); for BEAS-2B cells, the medium was removed and replaced with fresh complete BEGM medium containing 1 mM $CaCl_2$. ACT was added directly to cells and incubated for 30 min at 37°C. Cells were washed and lysed, and cAMP measured using the Tropix enzyme-linked immunosorbent assay (ELISA)-based cAMP assay kit (Applied Biosystems). For K562 cells, which grow in suspension, cells were spun down and resuspended in HBSS-HA. Toxin was added and the cells incubated at 37°C for 30 min, and cAMP measured as described above. Cell protein was measured, and data expressed as pmoles cAMP/mg cell protein. Under these time and temperature conditions, there is no cell death. *P* values were calculated by Student's two-tailed *t* test.

Experiments testing inhibition of cAMP generation by iACT. Catalytically inactive ACT (iACT) was generated by Osicka et al. (45) with a Cys-Thr insertion between amino acids 188 to 189 in the catalytic domain (kind gift from Peter Sebo, Institute of Microbiology, Prague, Czech Republic). This toxin mutant exhibits no AC enzyme activity but is equivalent to WT ACT in cell-binding characteristics by flow cytometry, hemolytic capability, and ability to induce potassium efflux (11, 14, 28, 45). For experiments testing inhibition of cAMP generation by the inactive ACT toxin mutant, 5,000 ng/ml (30 nM) iACT was added to cells for 5 min at room temperature prior to the addition of WT ACT. As a control for samples that received no iACT, a volume of 8 M urea (solution in which ACT is dissolved), equal to that used for the addition of iACT, was added. Cells were then incubated at 37°C for 30 min. We found that whether iACT was added for 5 min, for 15 min, at room temperature, or at 4°C, there was no difference in its ability to inhibit cAMP generation by WT ACT. For anti-CD11b, 20 μg/ml M1/70 antibody or isotype control was added to cells and incubated for 1 h at 4°C; ACT was then added and incubated at 37°C for 30 min.

Measurement of ACT association with cells. To measure cell-surface association of ACT by flow cytometry, adherent cells were removed from the tissue culture plate using cell dissociation buffer (Gibco) and washed. K562 cells were maintained in suspension and washed. Amounts of 1×10^6 cells were suspended in 100 μl HBSS plus 2% FBS. ACT was added to cells for 25 min at 37°C and the cells washed thoroughly at 4°C, and biotin-conjugated polyclonal anti-ACT antibody was added for 30 min at 4°C, followed by streptavidin-APC. Cells were then washed and fixed in 4% paraformaldehyde and assayed using a BD FACSCalibur and FlowJo analysis software. ACT binding was measured across the whole population of cells, rather than gating for high-CD11b- or CD18-expressing cells. Gating for high CR3 expression was not done in order to mimic conditions used for measuring cAMP and cell-associated adenylate cyclase enzymatic activity on adherent cells. Initial experiments using live/dead staining (Live/Dead fixable violet; Invitrogen) to identify and gate dead cells from flow cytometry analysis showed that there was no difference in binding measurements when cells were gated for forward- and side-scatter properties or for live/dead staining.

To determine if surface association of ACT (as measured by flow cytometry using our polyclonal antibody to ACT) changes over the time course used in these experiments, we added ACT to cells at 4°C for 10 min, washed them, and then moved the cells to 37°C for 15 or 30 additional minutes. Antibody to ACT was subsequently added at 4°C. We found that under these conditions, there was no loss of the ACT signal on the surface of cells (data not shown).

In addition to flow cytometry, the amount of ACT associated with cells was quantified by measuring the adenylate cyclase enzymatic activity of ACT-treated cells. CHO cells with and without CR3 were treated with cell dissociation buffer (Gibco) for 5 min at 37°C to detach them from tissue culture flasks. K562 (in suspension) or CHO cells were then spun down and washed twice in HBSS and resuspended to 1×10^6/ml. J774 cells were plated in 24-well tissue culture plates at 6×10^5 cells/well overnight in growth medium with 10% FBS-HI. ACT was added, and the cells incubated for 30 min at 37°C. The cells were then washed extensively at 4°C and lysed with 10 mM HEPES, pH 7.4, 150 mM NaCl, 10 mM EDTA, 4 mM EGTA, 1% Triton X-100 (lysis buffer). Twenty-microliter samples were assayed in the AC enzymatic assay (below). The background cellular adenylyl cyclase activity of untreated cells, which was minimal, was subtracted from the measurements to give the amount of AC enzyme associated with cells.

Measurement of AC enzymatic activity. AC enzymatic activity was measured by conversion of [α-^{32}P]ATP to [^{32}P]cAMP in a cell-free assay as described previously (18). Briefly, the reaction was carried out at 30°C and continued for 20 min in a final volume of 60 μl. Each assay contained 60 mM tricine, pH 8.0, 10 mM $MgCl_2$, 2 mM ATP (with 2×10^5 to 5×10^5 cpm of [α-^{32}P]ATP), and 1 μM calmodulin. The reaction was terminated by the addition of 100 μl of a solution containing 1% sodium dodecyl

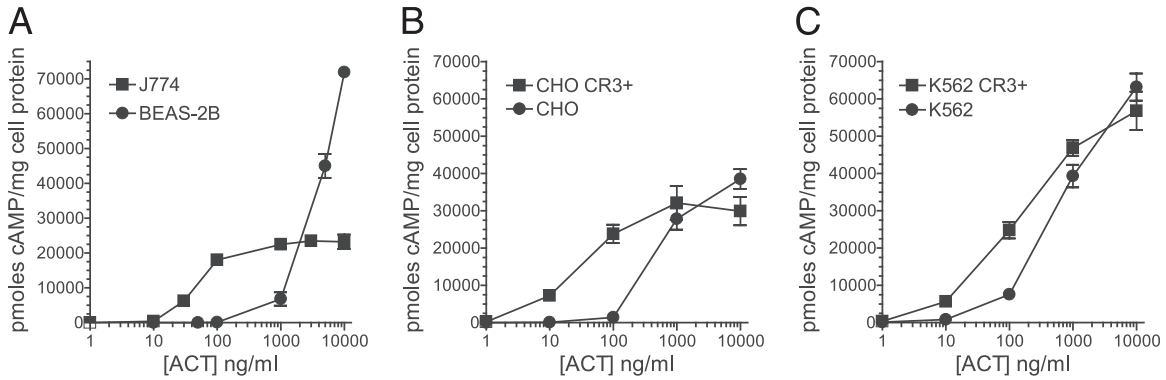

FIG 1 ACT-induced intracellular cAMP accumulation in cells with and without CR3. Each figure shows pmoles cAMP/mg of target cell protein as a function of toxin concentration. ACT was added to cells for 30 min at 37°C. (A) Accumulation of intracellular cAMP in J774 macrophage-like cells which express CR3 and in BEAS-2B epithelial cells which do not express CR3. Data presented are the means ± standard errors of duplicate samples in a single experiment which is representative of 3 individual experiments. (B) cAMP accumulation in CHO cells. Data presented are the means ± standard errors of 5 experiments each performed in triplicate. (C) cAMP accumulation in K562 cells. Data presented are the means ± standard errors of 6 experiments each performed in duplicate.

sulfate (SDS), 20 mM ATP, and 6.25 mM cAMP (including 15,000 to 20,000 cpm of [^{3}H]cAMP per tube for calculation of recovery). Cyclic AMP was quantified by the double column method of Salomon et al. (51).

Measurement of catalytic domain translocation. Samples were processed as described above for measurement of AC enzymatic assay, but before the lysis buffer was added, half of each sample was treated with 400 μg/ml trypsin for 10 min at 10°C and the reaction stopped with the addition of 800 μg/ml trypsin inhibitor. Control samples, reflecting total cell-associated ACT, were treated with trypsin inhibitor first and then trypsin. AC enzymatic activity was measured under both conditions, and the percentage of translocation of the catalytic domain into a trypsin-protected compartment was expressed as follows: 100 × (AC enzymatic activity in the trypsinized cell sample/AC enzymatic activity in the nontrypsinized control sample).

Quantification of intracellular ATP. Cells were prepared according to the protocol for measurement of cAMP. After incubation with ACT for 30 min at 37°C, cells were washed with PBS and lysed. Intracellular ATP was measured using the Perkin Elmer ATPlite luminescence ATP assay kit and read in a Perkin Elmer 1420 multilabel counter luminometer. For chemical depletion of ATP, 1 mM 2,4-dinitro-phenol (DNP) and 10 mM 2-deoxy-glucose (DOG) were added to cells for 60 min at 37°C prior to the addition of ACT. In experiments for comparing cAMP, ATP, and/or cell association, all of the assays were performed in parallel.

RESULTS

During the localized infection of the respiratory tract caused by *B. pertussis*, several specific cell types are exposed to ACT. Some of these, such as neutrophils and airway macrophages, express CD11b/CD18 (CR3) constitutively, while others, such as bronchial epithelial cells and lymphocytes, do not. *In vitro* examination of ACT-induced cAMP accumulation in these different cell types has revealed a pattern of response that is common to CR3-positive cells (CR3$^+$) and a different profile for CR3-negative (CR3$^-$) cells (Fig. 1). In J774 macrophages (CR3$^+$), for example, ACT-elicited cAMP accumulation is detected at 10 to 30 ng/ml ACT and reaches a plateau at between 100 and 1,000 ng/ml (Fig. 1A). In contrast, BEAS-2B bronchial epithelial cells are less sensitive to ACT but their cAMP accumulation increases steeply above 1,000 ng/ml ACT.

Because J774 and BEAS-2B cells differ in many aspects in addition to CR3 expression, we used two cell lines (Chinese hamster ovary [CHO] and K562 human erythroleukemic cells) which have been transfected to stably express CR3 and examined the role of CR3 in cAMP production. The expression of the integrin increases the potency of ACT in these cells, with a plateau in cAMP generation and intersection with the cAMP response curve of CR3$^-$ cells at ≥1,000 ng/ml (6 nM) ACT (Fig. 1B and C). The level of cAMP in CR3$^+$ cells is not significantly different from that in CR3$^-$ cells at 1,000 ng/ml ACT ($P = 0.46$, $n = 15$ for CHO cells, and $P = 0.052$, $n = 12$ for K562 cells) or at 10,000 ng/ml ($P = 0.064$, $n = 15$ for CHO cells, and $P = 0.32$, $n = 12$ for K562 cells). Thus, enhancement of cAMP generation by CR3 expression is limited, and at >1,000 ng/ml, ACT produces equivalent levels of cAMP in cells regardless of CR3 expression.

Bacterial toxins composed of a catalytic and a cell-binding domain utilize host cell glycoproteins and glycolipids as receptors for cell entry, and the presence of a specific receptor or receptor complex can be essential for the toxin to affect a specific target cell (12). For example, TEM8 was discovered as a receptor for protective antigen (PA) of *Bacillus anthracis* by mutagenesis of CHO-K1 cells that resulted in a 10,000-fold resistance to toxicity from lethal toxin (6, 52). Likewise, the potency of diphtheria toxin is reduced 10,000- to 100,000-fold in cells that do not express its receptor/coreceptor complex (heparin-binding epidermal growth factor [EGF]-like growth factor/CD9) (33, 42–44). Guermonprez et al. demonstrated that antibodies to CD11b can inhibit cAMP generation by ACT and that cells expressing the integrin are more sensitive to ACT (24). The toxin does not, however, require CR3 for intoxication, and little is known about the interaction between ACT and CR3$^-$ cells. To examine the specificity of the interaction between ACT and cells with and without CR3, we used a catalytically inactive form of ACT (iACT, constructed by Osicka et al. [45]) to compete with wild-type (WT) ACT and measured the generation of intracellular cAMP. The cell-binding and pore-forming properties of iACT, which differs from WT ACT by a 2-amino-acid insertion in the catalytic domain, are equivalent to those of WT ACT. As expected, the generation of intracellular cAMP by WT ACT in CHO CR3$^+$ cells is inhibited in the presence of a fixed concentration of iACT (5,000 ng/ml, 30 nM) (Fig. 2A). In contrast, iACT has no effect on cAMP generation by WT ACT in CR3$^-$ CHO cells (Fig. 2B). In K562 CR3$^+$ cells, iACT (5,000 ng/ml) inhibits cAMP generation by WT ACT at 10 ng/ml and 100 ng/ml to the levels of cAMP generated in K562 CR3$^-$ cells (Fig.

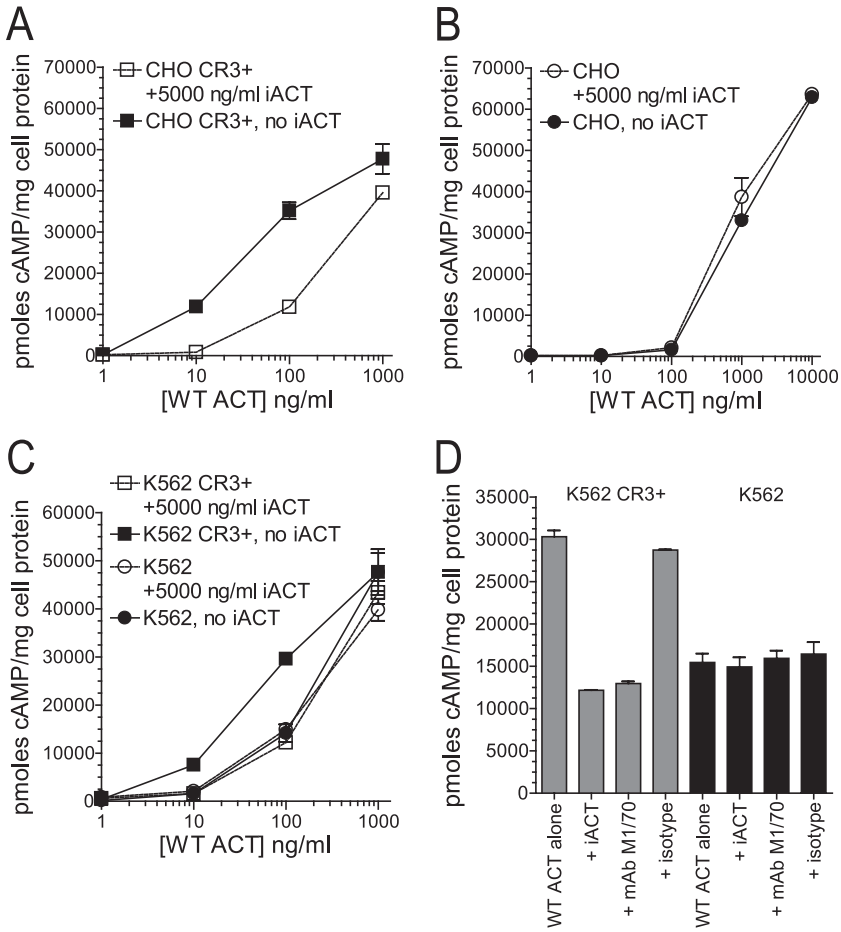

FIG 2 Competition with inactive ACT (iACT) decreases WT ACT-elicited cAMP accumulation in CHO CR3$^+$ and K562 CR3$^+$ cells but not in the respective control cells. (A) CHO CR3$^+$ cells were incubated with WT ACT at the specified concentrations in the continuous presence of 5,000 ng/ml (30 nM) iACT. (B) Same as described for panel A but with CHO control cells. (C) K562 CR3$^+$ (squares) and K562 control (circles) cells were incubated with WT ACT at the specified concentrations either without (closed) or with (open) 5,000 ng/ml iACT. (D) K562 CR3$^+$ (gray bars) and K562 (black bars) cells were incubated with 100 ng/ml WT ACT in the continuous presence of 5,000 ng/ml iACT. To examine blocking of cAMP generation by a MAb to CD11b, 100 ng/ml of ACT was added to cells after 1 h incubation at 4°C with 20 μg/ml MAb M1/70 to CD11b or 20 μg/ml isotype control antibody. Data presented are the means ± standard errors of duplicate samples in a single experiment which is representative of 3 (CHO) or 2 (K562) individual experiments.

2C). This concentration of iACT does not inhibit cAMP generation by WT ACT in K562 CR3$^-$ cells at any of the concentrations of WT ACT. There is no inhibition of ACT-induced cAMP accumulation when 1,000 ng/ml of WT ACT is added to K562 CR3$^+$ in the presence of 5,000 ng/ml of iACT. A monoclonal antibody to CD11b, clone M1/70, inhibits ACT-elicited cAMP (Fig. 2D) only in K562 CR3$^+$ cells. Together, these data show that the interaction between ACT and CR3$^+$ cells is competitively inhibited by catalytically inactive toxin but the interaction between ACT and CR3$^-$ cells is not.

To further examine this interaction between ACT and cells with and without CR3, we used two methods to measure binding. First, ACT was added to cells and surface-bound toxin was quantified by flow cytometry using polyclonal antibody to ACT (Fig. 3A). All experiments for measuring ACT binding were performed at 37°C in order to mimic the conditions under which intoxication occurs. Because endocytosis of cell-surface molecules is possible at 37°C, we used flow cytometry to test for loss of ACT from the cell surface at this temperature. When ACT was added to CR3$^+$ CHO or K562 cells at 4°C, cells were washed, and cell-associated ACT was measured after 0, 15, and 30 min at 37°C, there was no decrease over time in surface detection of ACT using polyclonal anti-ACT (data not shown). To complement the flow cytometric data, toxin binding to cells was quantified by the amount of AC enzymatic activity associated with the cells after incubation with ACT (29, 46) (Fig. 3B and C). In CHO cells, the level of binding to CR3$^+$ cells at 1,000 ng/ml was comparable to the level of binding to CR3$^-$ cells at 10,000 ng/ml (25,500 versus 23,200 units of cyclase activity). Similarly, the level of binding to CR3$^+$ K562 cells at 1,000 ng/ml was 7,280 units of cyclase activity, versus 5,750 in CR3$^-$ K562 cells at 10,000 ng/ml. At the highest concentration tested, 10,000 ng/ml, there was 2.4-fold greater binding to CR3$^+$ CHO cells than to CR3$^-$ CHO cells and 8.0-fold greater binding to CR3$^+$ K562 cells than to CR3$^-$ K562 cells. This difference in the enhancement of binding by CR3 may be related, in part, to the level of CR3 expression, which is greater in K562 cells than in CHO cells (Fig. 3E and D, respectively). Nevertheless, by both methods, there is greater binding of ACT to CR3$^+$ cells than to CR3$^-$ cells at all concentrations of ACT.

Since the step subsequent to cell binding involves translocation

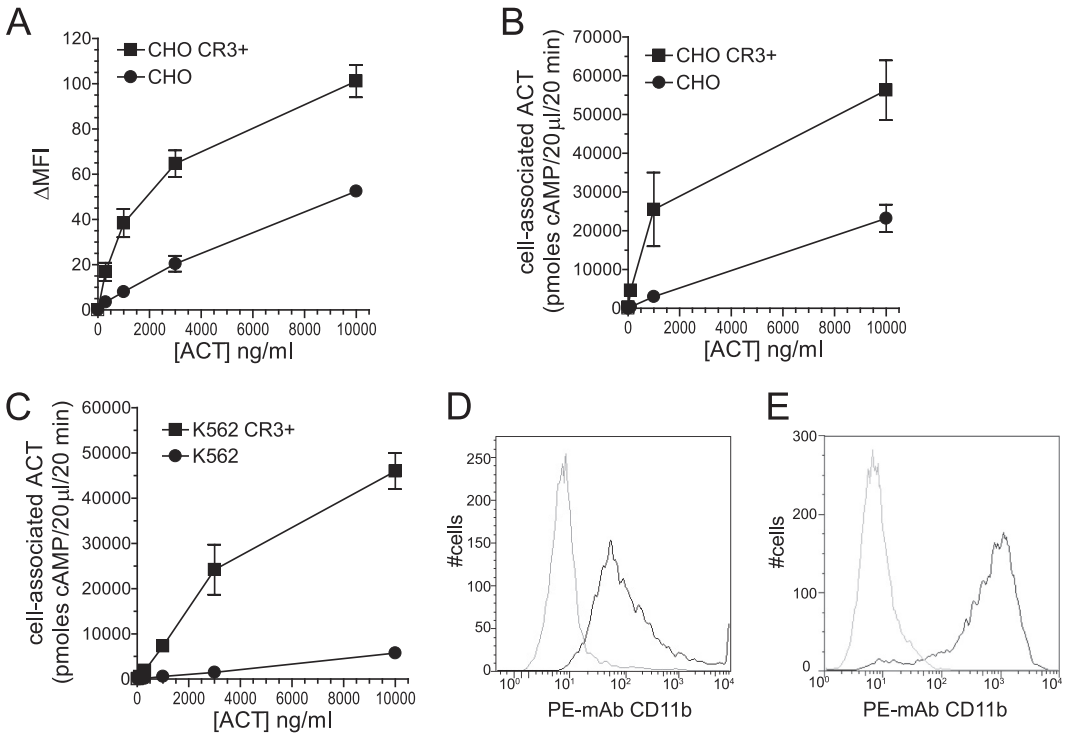

FIG 3 Association of ACT with cells is greater at all concentrations in the presence of CR3. (A) ACT was added to cells, unbound ACT was washed away, and biotin-conjugated polyclonal antibody to ACT, followed by APC-conjugated streptavidin, was added to detect surface-associated ACT. Results of flow cytometry measurements are expressed as difference in mean fluorescence intensity between cells not treated with toxin and those treated with toxin (ΔMFI). Data presented are the means ± standard errors of 3 separate experiments. (B, C) Total cell-associated ACT was measured by AC enzyme activity. Background native adenylyl cyclase activity, which is minimal, was subtracted from experimental conditions. Data presented are the means ± standard errors of 3 (CHO) or 2 (K562) experiments each performed in duplicate. (D) Surface expression of CD11b on CHO cells. CHO mock-transfected control cells (gray) and CHO CR3$^+$ cells (black) were stained with phycoerythrin-conjugated MAb to CD11b, clone ICRF44. Ten thousand cells were counted for each cell type. (E) Surface expression of CD11b on K562 cells. Conditions were the same as described for panel A but with K562 control cells (gray) and K562 CR3$^+$ cells (black). Ten thousand cells were counted for each cell type.

of the catalytic domain directly across the cytoplasmic membrane, we next tested whether CR3 affects this translocation, in addition to its enhancement of binding. As has been previously described (3, 15, 27, 29), catalytic domain translocation across the cytoplasmic membrane can be measured directly by adding ACT to cells at 37°C, washing cells to remove unbound ACT, and treating half of the cells with trypsin. The amount of AC enzymatic activity associated with cells after the addition of trypsin is compared to that associated with nontrypsinized cells (total cell-associated ACT) to determine the percentage of the bound toxin molecules that have translocated their catalytic domains into a trypsin-inaccessible compartment. CR3 expression increases the percentage of translocated toxin molecules (Fig. 4A and B) such that, at 10 to 500 ng/ml, ~80% of bound toxin molecules have translocated their catalytic domain in the presence of CR3 and ~25% in the absence of CR3. In CHO CR3$^+$ cells, the percentage of translocation decreases with increasing ACT concentration, eventually converging with that in CR3$^-$ CHO cells as the concentration of ACT is increased. In K562 cells, the amount of translocation is significantly greater in CR3$^+$ cells at all concentrations except for 10,000 ng/ml (Fig. 4B), and the percentages of translocation in CR3$^+$ (~80%) and CR3$^-$ cells (~25%) are similar to those seen in CHO cells.

These data show that both binding and translocation are enhanced by CR3 expression. There is, however, discordance between the toxin binding and resultant cAMP data in that binding is greater at all concentrations of toxin but cAMP values are equivalent in CR3$^+$ and CR3$^-$ cells at higher concentrations of ACT. It is, therefore, evident that, as the concentration of ACT is increased, more toxin binding does not result in proportionately more cAMP production. The binding of ACT to the cells over a range of concentrations can be expressed as area under the curve (AUC). The AUC for binding can be compared between CR3$^+$ and CR3$^-$ cells. In the case of K562 cells, the AUC for binding (Fig. 3C) is 2.8×10^8 for CR3$^+$ cells and 2.8×10^7 for CR3$^-$ cells (10-fold greater total binding to K562 CR3$^+$). On the other hand, the AUCs for cAMP generation in K562 CR3$^+$ and K562 CR3$^-$ cells (Fig. 1C, with calculation of AUC on a linear scale) are equivalent, 4.4×10^8 and 4.4×10^8, respectively. Thus, there is 10-fold greater binding in the presence of CR3, but the same amount of total cAMP generation. In CHO cells, the AUC for binding is 3.2-fold greater in CR3$^+$ cells than in CR3$^-$ cells (3.8×10^8 and 1.2×10^8, respectively) and the areas under the curve for cAMP are nearly equivalent (2.3×10^8 for CR3$^+$ cells and 2.6×10^8 for CR3$^-$ cells). In summary, despite enhanced binding and translocation in the presence of CR3, the generation of cAMP per unit of bound ACT in CR3$^+$ cells decreases as the amount of ACT bound to the cells increases.

We hypothesized that these findings are attributable to the next step in the process of cAMP generation after translocation, conversion of intracellular ATP to cAMP by the internalized enzy-

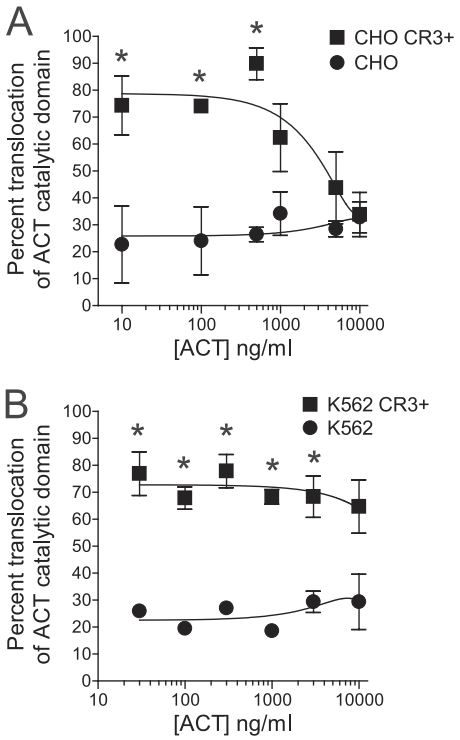

FIG 4 CR3 expression enhances translocation of the catalytic domain of ACT. (A) Percent translocation of the catalytic domain was calculated by adding ACT to CHO cells at 37°C, washing away unbound ACT, and treating half of the cells with trypsin. AC enzymatic activity was used to measure the amount of AC catalytic domain protected from trypsin (translocated to the cytosol) or the total amount of AC catalytic domain bound to nontrypsinized cells. Percent translocation was calculated as [AC enzyme in trypsinized sample/AC enzyme in nontrypsinized samples] × 100. (B) Percent translocation in K562 cells with or without CR3 was calculated. Data presented are the means ± standard errors of 4 (CHO) or 2 (K562) experiments each performed in duplicate. Translocation percentages for $CR3^+$ and $CR3^-$ cells were compared at each concentration, and an asterisk indicates a *P* value of <0.05 by Student's two-tailed *t* test. For concentrations not marked by an asterisk, the *P* value is >0.05.

matic domain. In our *in vitro* assay for enzymatic activity of purified toxin, 10 ng of toxin (with Mg^{2+} and calmodulin) can consume virtually all of the 2 mM ATP present in a sample in 20 min at 30°C. More importantly, ACT-mediated depletion of intracellular ATP occurs in cultured cells and contributes to cytotoxicity in macrophages (4, 28). Shown in Fig. 5A, in both CHO $CR3^+$ and CHO $CR3^-$ cells, ATP levels are reduced to <5% of those in untreated cells at 3,000 ng/ml of ACT. Intracellular cAMP levels were measured in parallel with ATP levels (Fig. 5B) and showed results comparable to those presented in Fig. 1B. When these data are represented as ATP depletion per unit of cAMP generated (Fig. 5C), it is evident that, at >60% ATP depletion, the production of cAMP by ACT is severely constrained. This suggests that ACT-induced depletion of intracellular ATP limits cAMP generation by ACT, resulting in a decrease in cAMP generation per unit of bound ACT in $CR3^+$ cells as the concentration of ACT is increased.

To ensure that this finding is not an artifact of the expression of CR3 in these transfected cell lines, we asked if ATP depletion limits cAMP generation in cells that express CR3 naturally. To do this, we measured ACT binding, cAMP accumulation, and ATP depletion in J774 macrophages. Under the conditions used for these experiments, there is no cell death. Treatment with 300 ng/ml ACT for 30 min results in an 89% reduction in ATP (Fig. 6A). To test whether this degree of ATP depletion affects the ability of ACT to raise intracellular cAMP levels, we reduced the cellular ATP concentration with 2-deoxy-glucose (DOG) and 2,4-dinitrophenol (DNP) prior to the addition of ACT. DOG is a glucose analog that inhibits glycolysis, and DNP is an uncoupler of oxidative phosphorylation in mitochondria (36, 41, 53, 56). DOG/DNP treatment results in an ATP concentration that is 15% ± 0.4% of that in untreated J774 cells. The subsequent addition of 30 ng/ml ACT to cells treated with DOG/DNP produced 616 pmol cAMP/mg cell protein, in comparison to 20,000 pmol cAMP/mg cell protein in untreated J774 cells (Fig. 6B)—a 97% reduction in cAMP production. Thus, the ability for ACT to generate cAMP is almost completely abolished with this magnitude of ATP depletion. Concordantly, cAMP generation in these cells plateaus at between 100 and 1,000 ng/ml ACT (Fig. 6C). With ATP substantially depleted and cAMP generation impaired at concentrations of >100 ng/ml ACT, the binding of ACT to J774 cells continues to increase with increasing concentrations of ACT (Fig. 6D). Plotting cAMP generation as a function of toxin binding reveals that as binding increases above ~22,000 units of cyclase activity (the amount of cell association at 300 ng/ml ACT), the ability for each

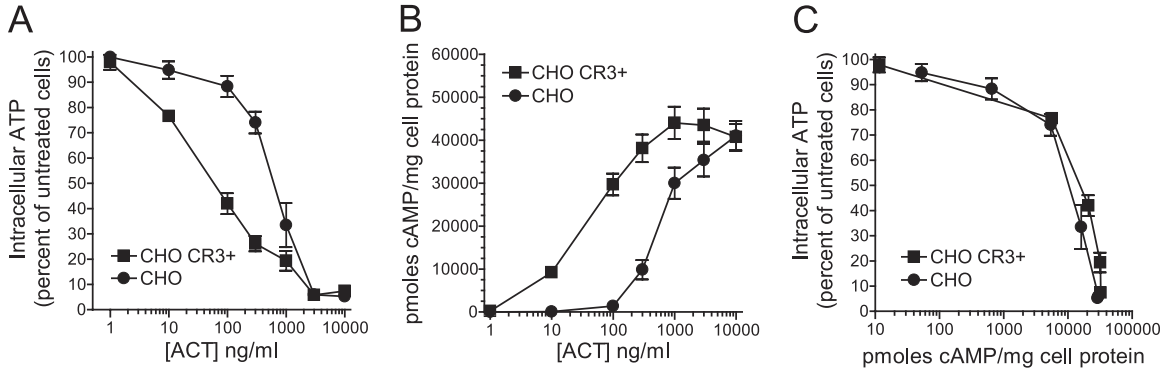

FIG 5 Cellular ATP depletion by ACT with and without CR3. ACT was added to cells at the indicated concentrations, and intracellular cAMP and ATP were measured on the same samples simultaneously after 30 min at 37°C. (A) Percentage of intracellular ATP was calculated for each sample with the formula (ATP in cells treated with ACT/baseline ATP in cells not treated with ACT) × 100. (B) Accumulation of intracellular cAMP in CHO cells measured in parallel with ATP. (C) ATP depletion as a function of cAMP generation, each measured in parallel. Data presented are the means ± standard errors of 3 experiments each performed in triplicate.

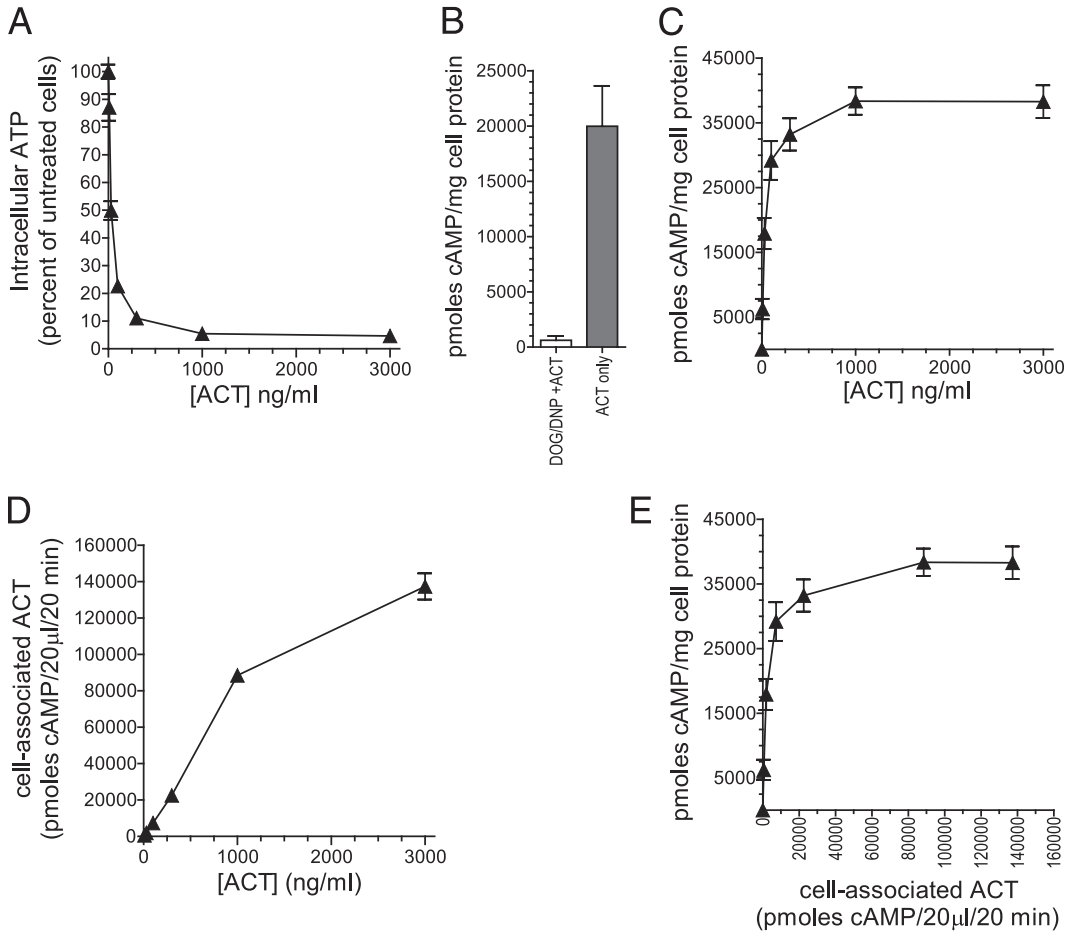

FIG 6 Comparison of ATP depletion, cAMP accumulation, and ACT-cell association in J774 cells. ACT was added to cells at the indicated concentrations, and intracellular cAMP, intracellular ATP, and cell-associated AC enzymatic activity were measured on the same samples simultaneously after 30 min at 37°C. (A) Intracellular ATP as a function of toxin concentration in J774 cells. Percentage of intracellular ATP was calculated for each sample with the formula (ATP in cells treated with ACT/baseline ATP in cells not treated with ACT) × 100. (B) Prior to addition of ACT, J774 cells were either untreated or treated with DNP/DOG which depleted ATP to 15% ± 0.4% of that in untreated cells. Subsequently, 30 ng/ml of ACT was added to cells for 30 min at 37°C and intracellular cAMP was measured. (C) Intracellular cAMP in J774 cells treated with the indicated concentrations of ACT. (D) Cell-associated ACT measured by AC enzymatic assay. (E) cAMP accumulation as a function of cell-associated ACT representing the amount of cAMP generated per unit of cell-associated ACT. Data presented are the means ± standard errors of 3 experiments each performed in triplicate.

additional unit of cell-associated ACT to generate cAMP is greatly diminished or eliminated. Like the CHO and K562 cells expressing CR3 by stable transfection, the amount of cAMP generated in J774 cells, which express physiologic levels of CR3, is not limited by the magnitude of cell association but by the availability of ATP. Interestingly, the levels of intracellular ATP in untreated BEAS-2B and J774 cells may explain, in part, why there is such a substantial difference in cAMP generated at 10,000 ng/ml ACT in these two cell types (Fig. 1A). Untreated BEAS-2B cells contain 380 ± 23 nmol intracellular ATP/mg cell protein, while J774 cells contain 11 ± 0.02 nmol intracellular ATP/mg cell protein.

DISCUSSION

The data presented here indicate that CR3 increases both the magnitude of binding and the percentage of ACT molecules that translocate their catalytic domains into the cytoplasm, resulting in increased potency of ACT. Importantly, $CR3^-$ cells accumulate cAMP when picomolar (100 ng/ml) concentrations of ACT are applied, and furthermore, the amount of accumulated cAMP in $CR3^-$ cells is equal to that in $CR3^+$ cells at low nanomolar concentrations (>1,000 ng/ml). Because the limit to ACT-induced cAMP accumulation is imposed by ATP depletion, the maximum amount of cAMP accumulation achieved in cells is not dependent on CR3 expression.

Approximately 60% ATP depletion severely constrains cAMP production by ACT (Fig. 5C). The consumption of ATP is probably the most significant factor limiting cAMP production in CHO $CR3^+$ cells, but additional toxin effects may contribute to the observed limitation as well. In CHO $CR3^+$ cells, there is a concentration-dependent decrease in translocation percentage at concentrations of ACT of >1,000 ng/ml. While this effect may contribute to the plateau in cAMP generation in CHO $CR3^+$ cells, we do not see this convergence in translocation in the K562 $CR3^+$ cells. It is, therefore, unlikely that the effect of CR3 on translocation fully accounts for the limit to cAMP accumulation. We have also tested whether cellular phosphodiesterase (PDE) inhibition with both 3-isobutyl-1-methylxanthine (IBMX) and dipyridamole (9) affects the limit to cAMP generation in $CR3^+$ and $CR3^-$

cells. These inhibitors do not significantly alter the profile of the cAMP concentration curves (data not shown). By measuring both intra- and extracellular cAMP generation by ACT, we have also concluded that cAMP efflux is not differentially affected by CR3 (data not shown). In agreement with the idea that PDEs and cAMP efflux do not account for cAMP limitation in $CR3^+$ cells, the amount of ATP consumed per cAMP generated (Fig. 5C) is equivalent in CHO $CR3^+$ and CHO $CR3^-$ cells across the range of concentrations tested.

Among the findings in this report, it is remarkable that CR3 enhances translocation by a similar percentage in both CHO and K562 cells (~80% translocation with CR3 and 25% without CR3) at concentrations of ACT of <1,000 ng/ml. At concentrations of ACT of >1,000 ng/ml, however, the translocation percentage in CHO $CR3^+$ cells decreases (Fig. 4), whereas this does not occur in K562 $CR3^+$ cells. This difference may be attributable to receptor expression levels, which are higher in K562 $CR3^+$ cells than in CHO $CR3^+$ cells (Fig. 3). If receptor binding favors translocation and if receptor-independent binding results in a lower likelihood of translocation, then, as CR3 receptors become occupied with increasing toxin concentrations, the percentage of translocation will become lower. With the greater receptor expression in K562 $CR3^+$ cells, receptor saturation would be expected to occur at higher concentrations of ACT than in CHO $CR3^+$ cells. In addition to expressing different levels of transfected receptor, the parent CHO and K562 cells are very different cell lines, probably with different cell surface lipid organization and protein components which may interact with CR3 to affect ACT translocation and oligomerization (7, 39, 57).

Our findings differ from the report by Guermonprez et al. in which CR3 was initially identified as a receptor for ACT. Their data show that, compared with parent CHO cells, CHO cells expressing CR3 exhibit greater intracellular cAMP accumulation at 5,000 ng/ml (24). In our studies using both CHO and K562 cells, we found equivalent cAMP accumulation in $CR3^+$ and $CR3^-$ cells within the range of 1,000 to 10,000 ng/ml of ACT. It is possible that the discrepancy lies in toxin potency and purity or in a difference in protocols for measurement of cAMP accumulation. Although it is difficult to identify a reason for the different findings between these reports, we do find concordant cAMP results in two different cell lines (Fig. 1), and our cAMP data are consistent with data regarding intracellular ATP depletion (Fig. 5).

The cellular effects of ACT have been studied across a wide range of concentrations in cells with and without CR3. The functional consequences of cAMP generation in CR3-positive cells, such as cell cycle arrest in J774 cells, are detectable at 1 ng/ml (22). In $CR3^-$ polarized epithelial cells, cAMP-induced chloride secretion results from the addition of <15 ng/ml ACT (11). On the other hand, cAMP-independent effects of ACT—oligomeric pore formation, induction of cellular potassium efflux, and stimulation of cellular calcium influx—have been identified using toxin concentrations that were often ≥1,000 ng/ml. Oligomerization of ACT in the membrane of cells has been observed, but the identification of oligomers has been possible only at concentrations of 25,000 to 48,000 ng/ml ACT (58). ACT induces potassium efflux upon initial contact with the cell membrane at concentrations of ≥1,000 ng/ml in sheep erythrocytes (21). However, Dunne et al. have recently demonstrated that 100 ng/ml ACT stimulates dendritic cells *in vitro* to secrete interleukin-1β (IL-1β), a function which is dependent on the ability for ACT to elicit potassium efflux (10). ACT induces cAMP-independent influx of extracellular calcium into the cytoplasm, but this is only detectable by calcium-sensitive dyes in CR3-positive cells at >5 nM (833 ng/ml) (14, 37). Calcium influx promotes endocytosis of ACT and membrane components in J774 cells, although in studies by Martin et al., only 4% of bound ACT was internalized at an ACT concentration of 1,670 ng/ml (39). The percentage of bound toxin that is internalized increases with toxin concentration, and most of these studies were performed using 5,830 ng/ml of ACT. On one hand, it is only possible to characterize cAMP-independent effects of ACT using catalytically inactive toxin. On the other hand, these cAMP-independent effects naturally occur in the setting of catalytically active, wild-type ACT. Thus, at the concentrations of ACT required to observe cAMP-independent effects, ATP depletion occurs in both $CR3^+$ and $CR3^-$ cells and will probably influence the outcomes and relevance of cAMP-independent effects.

The physiologic relevance of the effects of ACT, whether cAMP-dependent or independent, must be considered in the context of the cAMP generation, ATP depletion, and cytotoxicity potentially caused by the wild-type toxin. *In vitro*, ACT-induced cytotoxicity is dependent on the cell type and time course of toxin exposure. In J774 cells, 30 to 50 ng/ml of ACT after 2 h will cause cytotoxicity (28). On the other hand, cytotoxicity in CHO $CR3^+$ and K562 $CR3^+$ cells occurs in response to 1,000 ng/ml after 24 h but not after 2 h of exposure to ACT (data not shown). Even more resistant to killing by ACT, BEAS-2B cells exhibit no lactate dehydrogenase release after treatment with 1,000 ng/ml of ACT for 24 h (data not shown). Furthermore, the type of cell death is affected by the levels of cAMP and ATP. J774 cells die by cAMP-induced, noninflammatory apoptosis in response to concentrations of ACT that do not deplete ATP, but they die by a potentially proinflammatory, nonapoptotic cell death from concentrations that deplete ATP (28). Thus, a concentration of ACT that fully depletes ATP is not uniformly fatal to cells, and so, functions of ACT that are only observed at "high" concentrations of ACT that fully deplete ATP may be physiologically relevant in certain cells.

Although the levels of ACT present in the airway during infection with *B. pertussis* are not known, it is likely that the concentrations are sufficient to affect $CR3^-$ cells, such as respiratory epithelial cells, that may have several hundred bacteria attached. We have demonstrated that polarized epithelial cells respond to <15 ng/ml of ACT with chloride efflux into the luminal space (11). In addition, IL-2 secretion from activated T cells and T-cell proliferation are impaired by 23 and 46 ng/ml of ACT, respectively (47, 50). Interestingly, Paccani et al. have recently shown that ACT interacts with LFA-1, another β2 integrin, on T cells, and this may account for their sensitivity to ACT (48).

Since the identification of ACT by serendipitous recognition of AC activity in vaccine preparations, it has become clear that the toxin exhibits multiple functions, both cAMP dependent and independent. The concentration dependence of all of these effects has only partially been characterized, with the cAMP-independent effects occurring at a higher range of ACT concentrations than the cAMP-dependent effects. The role that CR3 plays in each of these functions is also not well understood. Here, we have characterized the concentration dependence of ACT-elicited cAMP accumulation, which occurs over a broad range of ACT concentrations when compared to other ACT effects, and found that CR3 does not simply shift the cAMP concentration curve to the left but also changes the nature of the process of cAMP generation by provid-

ing a receptor-based mode of intoxication in addition to a nonreceptor-based mechanism and by enhancing catalytic domain translocation in comparison to that in cells without CR3. Thus, to fully understand ACT-cell interaction, it is important to study cells both with and without CR3. Through characterizing the concentration dependence of ACT activity, we found that ATP limits cAMP accumulation in a CR3-independent manner. ATP depletion must, therefore, be considered when interpreting the effects of ACT in cells both with and without CR3.

ACKNOWLEDGMENTS

This work was supported by funding from NIH, NIAID (grants 5 R01 AI018000 [E.L.H.] and 1K08AI081900-01 [J.C.E.]).

REFERENCES

1. **Bachelet M, Richard MJ, Francois D, Polla BS.** 2002. Mitochondrial alterations precede Bordetella pertussis-induced apoptosis. FEMS Immunol. Med. Microbiol. **32**:125–131.
2. **Barry EM, et al.** 1991. Bordetella pertussis adenylate cyclase toxin and hemolytic activities require a second gene, cyaC, for activation. J. Bacteriol. **173**:720–726.
3. **Basler M, et al.** 2007. Segments crucial for membrane translocation and pore-forming activity of Bordetella adenylate cyclase toxin. J. Biol. Chem. **282**:12419–12429.
4. **Basler M, Masin H, Osicka R, Sebo P.** 2006. Pore-forming and enzymatic activities of Bordetella pertussis adenylate cyclase toxin synergize in promoting lysis of monocytes. Infect. Immun. **74**:2207–2214.
5. **Benz R, Maier E, Ladant D, Ullmann A, Sebo P.** 1994. Adenylate-cyclase toxin (CyaA) of Bordetella pertussis. Evidence for the formation of small ion-permeable channels and comparison with HlyA of Escherichia coli. J. Biol. Chem. **269**:27231–27239.
6. **Bradley KA, Mogridge J, Mourez M, Collier RJ, Young JA.** 2001. Identification of the cellular receptor for anthrax toxin. Nature **414**:225–229.
7. **Bumba L, Masin J, Fiser R, Sebo P.** 2010. Bordetella adenylate cyclase toxin mobilizes its beta(2) integrin receptor into lipid rafts to accomplish translocation across target cell membrane in two steps. PLoS Pathog. **6**:e1000901.
8. **Confer DL, Eaton JW.** 1982. Phagocyte impotence caused by an invasive bacterial adenylate cyclase. Science **217**:948–950.
9. **Dong HL, Osmanova V, Epstein PM, Brocke S.** 2006. Phosphodiesterase 8 (PDE8) regulates chemotaxis of activated lymphocytes. Biochem. Biophys. Res. Commun. **345**:713–719.
10. **Dunne A, et al.** 2010. Inflammasome activation by adenylate cyclase toxin directs Th17 responses and protection against Bordetella pertussis. J. Immunology **185**:1711–1719.
11. **Eby JC, et al.** 2010. Selective translocation of the Bordetella pertussis adenylate cyclase toxin across the basolateral membranes of polarized epithelial cells. J. Biol. Chem. **285**:10662–10670.
12. **Eidels L, Proia RL, Hart DA.** 1983. Membrane receptors for bacterial toxins. Microbiol. Rev. **47**:596–620.
13. **El-Azami-El-Idrissi M, et al.** 2003. Interaction of *Bordetella pertussis* adenylate cyclase with CD11b/CD18: role of toxin acylation and identification of the main integrin interaction domain. J. Biol. Chem. **278**:38514–38521.
14. **Fiser R, et al.** 2007. Third activity of Bordetella adenylate cyclase (AC) toxin-hemolysin. Membrane translocation of AC domain polypeptide promotes calcium influx into CD11b+ monocytes independently of the catalytic and hemolytic activities. J. Biol. Chem. **282**:2808–2820.
15. **Friedman E, Farfel Z, Hanski E.** 1987. The invasive adenylate cyclase of Bordetella pertussis. Properties and penetration kinetics. Biochem. J. **243**:145–151.
16. **Glaser P, et al.** 1988. The calmodulin-sensitive adenylate cyclase of Bordetella pertussis: cloning and expression in Escherichia coli. Mol. Microbiol. **2**:19–30.
17. **Glaser P, Sakamoto H, Bellalou J, Ullmann A, Danchin A.** 1988. Secretion of cyclolysin, the calmodulin-sensitive adenylate cyclase-haemolysin bifunctional protein of *Bordetella pertussis*. EMBO J. **7**:3997–4004.
18. **Goldhammer AR, et al.** 1981. Spurious protein activators of *Bordetella pertussis* adenylate cyclase. Eur. J. Biochem. **115**:605–609.
19. **Gordon VM, Leppla SH, Hewlett EL.** 1988. Inhibitors of receptor-mediated endocytosis block the entry of *Bacillus anthracis* adenylate cyclase toxin but not that of *Bordetella pertussis* adenylate cyclase toxin. Infect. Immun. **56**:1066–1069.
20. **Gordon VM, et al.** 1989. Adenylate cyclase toxins from *Bacillus anthracis* and *Bordetella pertussis*. Different processes for interaction with and entry into target cells. J. Biol. Chem. **264**:14792–14796.
21. **Gray M, Szabo G, Otero AS, Gray L, Hewlett E.** 1998. Distinct mechanisms for K+ efflux, intoxication, and hemolysis by *Bordetella pertussis* AC toxin. J. Biol. Chem. **273**:18260–18267.
22. **Gray MC, Hewlett EL.** 2011. Cell cycle arrest induced by the bacterial adenylate cyclase toxins from Bacillus anthracis and Bordetella pertussis. Cell. Microbiol. **13**:123–134.
23. **Gray MC, et al.** 2001. Translocation-specific conformation of adenylate cyclase toxin from *Bordetella pertussis* inhibits toxin-mediated hemolysis. J. Bacteriol. **183**:5904–5910.
24. **Guermonprez P, et al.** 2001. The adenylate cyclase toxin of *Bordetella pertussis* binds to target cells via the $\alpha M\beta 2$ (integrin CD11b/CD18). J. Exp. Med. **193**:1035–1044.
25. **Guermonprez P, Ladant D, Karimova G, Ullmann A, Leclerc C.** 1999. Direct delivery of the Bordetella pertussis adenylate cyclase toxin to the MHC class I antigen presentation pathway. J. Immunol. **162**:1910–1916.
26. **Hackett M, Guo L, Shabanowitz J, Hunt DF, Hewlett EL.** 1994. Internal lysine palmitoylation in adenylate cyclase toxin from Bordetella pertussis. Science **266**:433–435.
27. **Hanski E, Farfel Z.** 1985. Bordetella pertussis invasive adenylate cyclase. Partial resolution and properties of its cellular penetration. J. Biol. Chem. **260**:5526–5532.
28. **Hewlett EL, Donato GM, Gray MC.** 2006. Macrophage cytotoxicity produced by adenylate cyclase toxin from Bordetella pertussis: more than just making cyclic AMP! Mol. Microbiol. **59**:447–459.
29. **Hewlett EL, et al.** 1993. Characterization of adenylate cyclase toxin from a mutant of *Bordetella pertussis* defective in the activator gene cyaC. J. Biol. Chem. **268**:7842–7848.
30. **Hickey FB, Brereton CF, Mills KH.** 2008. Adenylate cyclase toxin of Bordetella pertussis inhibits TLR-induced IRF-1 and IRF-8 activation and IL-12 production and enhances IL-10 through MAPK activation in dendritic cells. J. Leukoc. Biol. **84**:234–243.
31. **Ingalls RR, Arnaout MA, Golenbock DT.** 1997. Outside-in signaling by lipopolysaccharide through a tailless integrin. J. Immunol. **159**:433–438.
32. **Iwaki M, Ullmann A, Sebo P.** 1995. Identification by in vitro complementation of regions required for cell-invasive activity of *Bordetella pertussis* adenylate cyclase toxin. Mol. Microbiol. **17**:1015–1024.
33. **Iwamoto R, Senoh H, Okada Y, Uchida T, Mekada E.** 1991. An antibody that inhibits the binding of diphtheria toxin to cells revealed the association of a 27-kDa membrane protein with the diphtheria toxin receptor. J. Biol. Chem. **266**:20463–20469.
34. **Kamanova J, et al.** 2008. Adenylate cyclase toxin subverts phagocyte function by RhoA inhibition and unproductive ruffling. J. Immunol. **181**:5587–5597.
35. **Lee SJ, Gray MC, Guo L, Sebo P, Hewlett EL.** 1999. Epitope mapping of monoclonal antibodies against Bordetella pertussis adenylate cyclase toxin. Infect. Immun. **67**:2090–2095.
36. **Lieberthal W, Menza SA, Levine JS.** 1998. Graded ATP depletion can cause necrosis or apoptosis of cultured mouse proximal tubular cells. Am. J. Physiol. **274**(2 Pt 2):F315–F327.
37. **Martin C, Gomez-Bilbao G, Ostolaza H.** 2010. Bordetella adenylate cyclase toxin promotes calcium entry into both CD11b(+) and CD11b(-) cells through cAMP-dependent L-type-like calcium channels. J. Biol. Chem. **285**:357–364.
38. **Martin C, et al.** 2004. Membrane restructuring by Bordetella pertussis adenylate cyclase toxin, a member of the RTX toxin family. J. Bacteriol. **186**:3760–3765.
39. **Martin C, Uribe KB, Gomez-Bilbao G, Ostolaza H.** 2011. Adenylate cyclase toxin promotes internalisation of integrins and raft components and decreases macrophage adhesion capacity. PLoS One **6**:e17383.
40. **Masin J, Konopasek I, Svobodova J, Sebo P.** 2004. Different structural requirements for adenylate cyclase toxin interactions with erythrocyte and liposome membranes. Biochim. Biophys. Acta **1660**:144–154.
41. **Matheson BK, Adams JL, Zou J, Patel R, Franklin RB.** 2007. Effect of

metabolic inhibitors on ATP and citrate content in PC3 prostate cancer cells. Prostate **67**:1211–1218.
42. **Middlebrook JL, Dorland RB, Leppla SH.** 1978. Association of diphtheria toxin with Vero cells. Demonstration of a receptor. J. Biol. Chem. **253**:7325–7330.
43. **Mitamura T, et al.** 1992. The 27-kD diphtheria toxin receptor-associated protein (DRAP27) from Vero cells is the monkey homologue of human CD9 antigen: expression of DRAP27 elevates the number of diphtheria toxin receptors on toxin-sensitive cells. J. Cell Biol. **118**:1389–1399.
44. **Naglich JG, Metherall JE, Russell DW, Eidels L.** 1992. Expression cloning of a diphtheria toxin receptor: identity with a heparin-binding EGF-like growth factor precursor. Cell **69**:1051–1061.
45. **Osicka R, et al.** 2000. Delivery of $CD8^+$ T-cell epitopes into major histocompatibility complex class I antigen presentation pathway by *Bordetella pertussis* adenylate cyclase: delineation of cell invasive structures and permissive insertion sites. Infect. Immun. **68**:247–256.
46. **Osickova A, Osicka R, Maier E, Benz R, Sebo P.** 1999. An amphipathic α-helix including glutamates 509 and 516 is crucial for membrane translocation of adenylate cyclase toxin and modulates formation and cation selectivity of its membrane channels. J. Biol. Chem. **274**:37644–37650.
47. **Paccani SR, et al.** 2008. Suppression of T-lymphocyte activation and chemotaxis by the adenylate cyclase toxin of Bordetella pertussis. Infect. Immun. **76**:2822–2832.
48. **Paccani SR, et al.** 2011. The Bordetella pertussis adenylate cyclase toxin binds to T cells via LFA-1 and induces its disengagement from the immune synapse. J. Exp. Med. **208**:1317–1330.
49. **Pearson RD, Symes P, Conboy M, Weiss AA, Hewlett EL.** 1987. Inhibition of monocyte oxidative responses by *Bordetella pertussis* adenylate cyclase toxin. J. Immunol. **139**:2749–2754.
50. **Rossi Paccani S, et al.** 2009. The adenylate cyclase toxins of Bacillus anthracis and Bordetella pertussis promote Th2 cell development by shaping T cell antigen receptor signaling. PLoS Pathog. **5**:e1000325.
51. **Salomon Y, Londos C, Rodbell M.** 1974. A highly sensitive adenylate cyclase assay. Anal. Biochem. **58**:541–548.
52. **Scobie HM, Rainey GJ, Bradley KA, Young JA.** 2003. Human capillary morphogenesis protein 2 functions as an anthrax toxin receptor. Proc. Natl. Acad. Sci. U. S. A. **100**:5170–5174.
53. **Sorensen M, Sehested M, Jensen PB.** 1999. Effect of cellular ATP depletion on topoisomerase II poisons. Abrogation of cleavable-complex formation by etoposide but not by amsacrine. Mol. Pharmacol. **55**:424–431.
54. **Spensieri F, et al.** 2006. Bordetella pertussis inhibition of interleukin-12 (IL-12) p70 in human monocyte-derived dendritic cells blocks IL-12 p35 through adenylate cyclase toxin-dependent cyclic AMP induction. Infect. Immun. **74**:2831–2838.
55. **Szabo G, Gray MC, Hewlett EL.** 1994. Adenylate cyclase toxin from *Bordetella pertussis* produces ion conductance across artificial lipid bilayers in a calcium- and polarity-dependent manner. J. Biol. Chem. **269**:22496–22499.
56. **Terada H.** 1990. Uncouplers of oxidative phosphorylation. Environ. Health Perspect. **87**:213–218.
57. **Vojtova J, Kofronova O, Sebo P, Benada O.** 2006. Bordetella adenylate cyclase toxin induces a cascade of morphological changes of sheep erythrocytes and localizes into clusters in erythrocyte membranes. Microsc. Res. Tech. **69**:119–129.
58. **Vojtova-Vodolanova J, et al.** 2009. Oligomerization is involved in pore formation by Bordetella adenylate cyclase toxin. FASEB J. **23**:2831–2843.
59. **Xiong YM, Chen J, Zhang L.** 2003. Modulation of CD11b/CD18 adhesive activity by its extracellular, membrane-proximal regions. J. Immunol. **171**:1042–1050.